

Active Self-Assembled Monolayer Sensors for Trace Explosive Detection

Mingliang Li,[#] Hongliang Chen,[#] Shuo Li, Guozhi Wang, Feng Wei, Xuefeng Guo,^{*} and Hailing Tu^{*}



Cite This: *Langmuir* 2020, 36, 1462–1466



Read Online

ACCESS |



Metrics & More

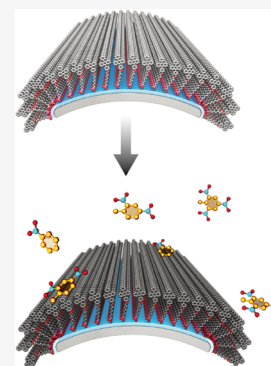


Article Recommendations



Supporting Information

ABSTRACT: Trace explosives can be detected with the help of a portable device using a flexible active self-assembled monolayer (SAM). 9,10-diphenyl anthracene with aggregation-induced emission enhancement (AIEE) properties is selected as the fluorophore. Phosphoric acid as the anchor group is linked to the fluorophore through an alkyl chain and able to self-assemble into a dense monolayer on the HfO₂ adhesion layer on a flexible substrate. The dense SAMs show high fluorescence intensity, which can be quenched by nitroaromatic compounds (NACs), and have advantages of high response rate, sensitivity, reversibility, and selectivity.



INTRODUCTION

Much attention has been paid to the detection of explosive compounds in antiterrorism applications. Many analytical techniques have been developed to detect traces of high explosives, such as nitroaromatic compounds (NACs). However, most of them require large, lab-based analytical instruments such as high-performance liquid chromatography (HPLC), mass spectrometry (MS), UV absorption detectors, and X-ray imaging.¹ Among all of the techniques, fluorescence sensors, with the benefits of simplicity, low cost, and high sensitivity, have attracted broad application prospects.² Among the fluorescent probes, conjugated polymers are one of the most promising candidates for explosive detection with high sensitivity at the ppm level,^{3–5} which can be attributed to the molecular wire effect,⁶ enabling the rapid propagation of an exciton throughout the individual polymer chain.^{7,8} Some shortcomings, however, undermine their wide application as an explosive gas sensor, such as large film thickness that can reduce detection sensitivity,⁹ easy aggregation that cuts down the fluorescent luminous efficiency,¹⁰ and poor solvent intolerance that results in poor stability in further process and service.¹¹ Small-molecule chromophores have definite structures and can self-assemble into highly ordered superstructures. Their fluorescence, however, only exists in the dispersed state; their emission is greatly quenched at higher concentrations or aggregated/solid state, which can be attributed to the aggregation-caused quenching (ACQ) behaviors.^{12–14} Thus, the fabrication of high-fluorescence, solid-state film sensors from these chromophores becomes highly untenable. In 2001, Tang et al. observed an opposite phenomenon to the ACQ, in which fluorophores were faintly

emissive in the molecularly dissolved state but strongly emissive in the aggregated state and this observation is termed the aggregation-induced emission enhancement (AIEE).^{15,16} AIEE-active materials are regarded as an ideal solution for the above-mentioned issue.

In this study, we designed a densely packed self-assembled monolayer (SAM) flexible sensor to detect NACs based on fluorescence quenching of an AIEE-active fluorophore (Figure 1). The sensing layer was fabricated with a newly designed functional small-molecule PA-2PhAn, wherein the fluorophore was 9,10-diphenyl anthracene with AIEE properties (Figure S7)¹⁷ and phosphoric acid was used as an anchor group¹⁸ linking to the fluorophore via an alkyl chain (Figure 1B top). As the AIEE fluorophore group can alleviate the problem of fluorescence quenching caused by the aggregation of the polymer, the formation of a dense SAM can still ensure fluorescence intensity (Figure 1C).¹⁹ Moreover, the self-assembled monolayer is sensitive as a sensing layer.²⁰ Phosphoric acid as an anchor group can form a covalent bond with the HfO₂ adhesion layer to improve material stability. The SAMs manufactured on flexible substrates provide an experimental basis for the preparation of flexible sensors (Figure 1D) and the development of wearable devices (Figures 1A and 2B down).

Received: December 5, 2019

Revised: January 25, 2020

Published: January 28, 2020

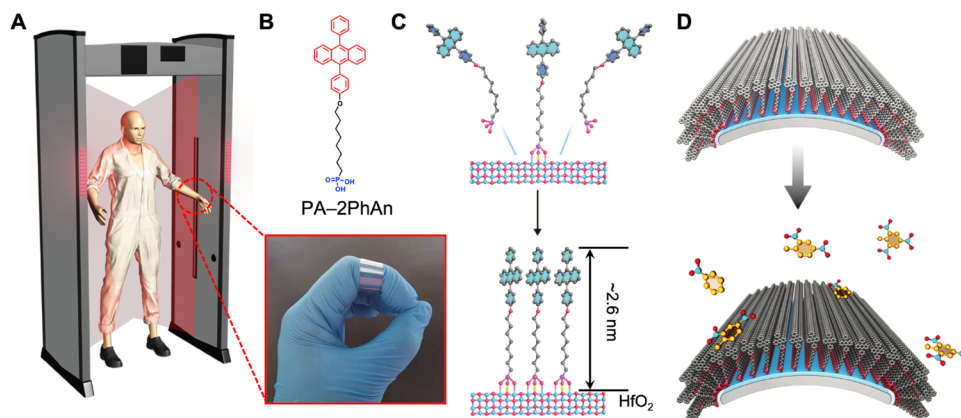


Figure 1. (A) SAM sensors for trace NACs in the security check. (B) Molecular structure of PA-2PhAn (top) and the SAM sensor on the poly(ethylene terephthalate) (PET) substrate (down). (C) Schematic cross section of the formation of the PA-2PhAn SAM on the HfO₂ adhesion layer. (D) Quenching model of the flexible SAM sensor by NACs.

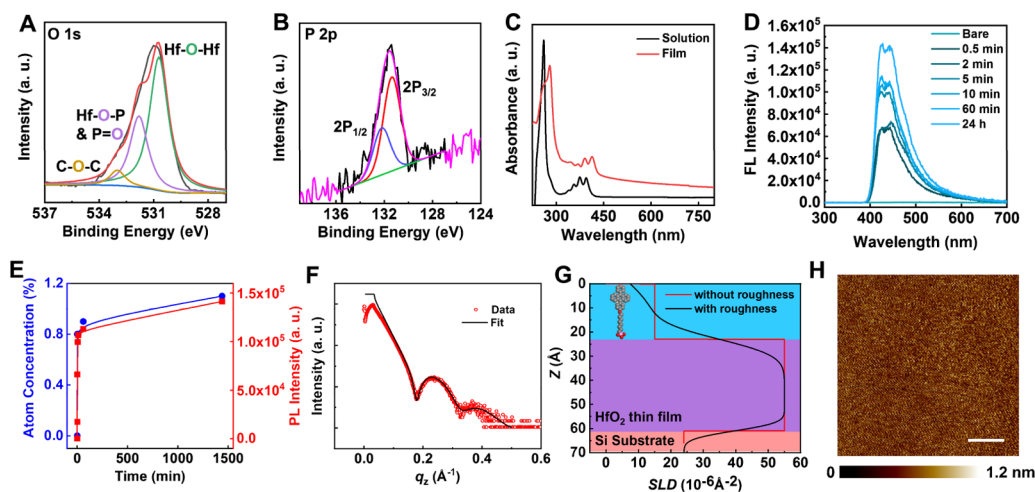


Figure 2. Characterization of the SAM/HfO₂ interface. High-resolution X-ray photoelectron spectroscopy (XPS) for (A) O 1s and (B) P 2p. (C) UV-vis absorption of PA-2PhAn in solution (black) and solid-state thin films on quartz substrates (red). (D) Fluorescence intensity with increasing the assembling time ($\lambda_{\text{ex}} = 263.00$ nm). (E) Atomic concentration of phosphorus in PA-2PhAn SAM (blue) and the fluorescence counts ($\lambda_{\text{em}} = 450.00$ nm) with increasing the assembling time. (F) X-ray reflectivity (XRR) measurement of the SAM with a HfO₂ thin film on a silicon substrate (red dots) and the corresponding fitting curve (black curve). (G) Scattering length density (SLD) profile with (black curve) and without (red curve) roughness. (H) Atomic force microscopy (AFM) topography image of PA-2PhAn SAM on the ALD HfO₂ surface.

Assembling of PA-2PhAn SAM. A qualified film was prepared by immersing the substrate in a PA-2PhAn solution^{21–23} (procedures are shown in Figure S2). To confirm the linkage of PA-2PhAn molecules to the HfO₂ layer, the contact angle was determined and X-ray photoelectron spectroscopy (XPS) was performed. In Figure S4, the contact angle increased from an acute angle (53.13, 51.74°) to an obtuse angle (108.99, 109.07°), which proved that the linkage with PA-2PhAn made the HfO₂ surface hydrophobic. From high-resolution XPS studies (Figure 2A), we found that the O 1s signals could be fitted with three components, 530.7, 531.8, and 533.1 eV. These components can be assigned to Hf–O–Hf, Hf–O–P (or P = O of the phosphonate group), and C–O–C, respectively.²⁴ In combination with the appearance of P 2p signals (Figure 2B), these results revealed the successful attachment of PA-2PhAn molecules onto the HfO₂ surface by covalent bonds. Ultraviolet–visible spectra (UV-vis, Figure 2C) show the aggregation of PA-2PhAn, as the initial absorption point in solution is about 20 nm lower to the low field compared to that in solid-state thin films. In addition, in Figure 2D, the fluorescence spectrum tail past 500

nm represents the chromophore excimer fluorescence, which further proves the aggregation.²⁵ However, aggregation does not quench the fluorescence. Figure 2D shows that longer assembling time leads to stronger fluorescence intensities. The peak counts at $\lambda_{\text{em}} = 450.00$ nm and the element concentration of phosphorus from time-resolved, high-resolution XPS (Figure S5) were extracted and are presented in Figure 2E. They both increase over time, which means longer growth time helps to form more compact and denser films with stronger fluorescence intensities due to the molecular absorption and AIEE effect. When the concentration of phosphorus and the fluorescence intensity tend to be stable by 60 min, a robust SAM formed. Low-angle X-ray reflectivity (XRR) was used to illustrate the formation of a SAM in a highly dense manner (Figures 2F and S3 and Table S1). The scattering length density (SLD) profile provided further evidence of the homogeneous assembly of the monolayer (Figure 2G), which could be modeled as a two-layer structure with different electron densities: a PA-2PhAn layer (approximately 2.3 nm) and a HfO₂ layer (approximately 3.8 nm). This fit yielded a monolayer thickness of approximately 2.3 nm, which was

consistent with a real-space model of PA-2PhAn (ca. 2.6 nm in Figure 1B). Moreover, SAM fabrication did not increase the roughness, as indicated by the atomic force microscopy (AFM, Figure 2H) image.

Excitation and emission spectra were recorded at different analysis wavelengths or different excitation wavelengths, as shown in Figure 3A. According to Kasha's rule,²⁶ it is supposed

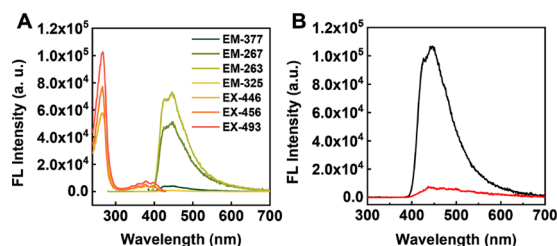


Figure 3. (A) Fluorescence excitation and emission spectra of the PA-2PhAn SAMs recorded at various excitation and analysis wavelengths. (B) Fluorescence quenching of the PA-2PhAn SAMs examined in nitrobenzene-saturated air.

that PA-2PhAn has a homogeneous distribution on the substrate surface as the profiles of the two spectra are independent of analysis wavelength or excitation wavelength. All quenching calculations were from the maximum emission measurements of each fluorescence spectrum, and all of the emission spectra were conducted at $\lambda_{\text{ex}} = 263.00$ nm, where the strongest fluorescence intensity was produced.

To avoid the effect of evaporation on the sensing performance of the devices, 0.2 mL of nitrobenzene (NB) was dropped onto the bottom of the specially designed apparatus (Figure S1) and kept it for 10 min for the stable saturate evaporation. The film was inserted for 5 min for complete quenching. In Figure 3b, clearly, the response is almost instantaneous and the quenching efficiency reaches 93.49%, according to eq S1.

Quenching Mechanism of the SAM Sensor. More detailed quenching experiments were conducted. Figure 4A

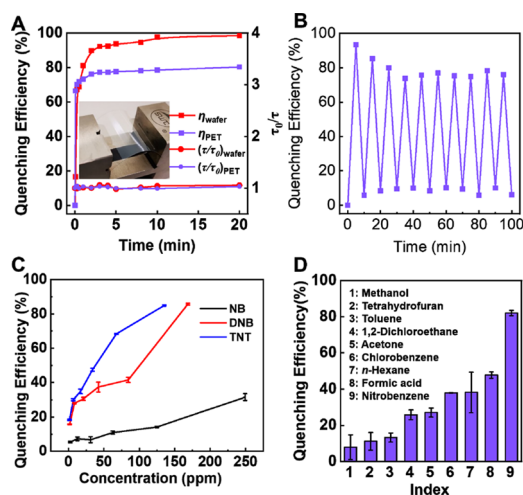


Figure 4. (A) Quenching efficiency and τ/τ_0 as a function of exposure time in NB for SAMs both on the silicon wafer and flexible PET. The inset shows an image of the flexible SAM sensor on PET substrates. (B) Reversibility of the SAM sensors. (C) Concentration dependence of the quenching efficiency in different NACs for 10 s. (D) Selectivity of the SAM sensors. Intensities were extracted at $\lambda_{\text{em}} = 450.00$ nm.

shows the plots of the quenching efficiency and τ/τ_0 as a function of time in NB vapor on both flexible PET and silicon wafer, where τ_0 and τ stand for the original and real-time lifetimes (as shown in Tables S3 and S4). We can see that it takes about 4 min for the emission of the film to reach the equilibrium and the equilibrium fluorescence quenching efficiency of silicon wafer devices is higher than that of flexible PET, which is ca. 93% for silicon wafer devices and ca. 77% for flexible PET. The reason for the differences is that the curved surface of PET and the coarse sol-gel-prepared HfO_2 layer made the anchored PA-2PhAn molecules less compact compared to the flat hard silicon wafer and the flat ALD HfO_2 layer because of the lower degree of molecular conjugation and the smaller size of the π plane with the bigger angles between the benzene and anthracene. However, the flexible sensors can still maintain relatively high yield with stable quenching efficiency, which facilitates further applications. The quenching mechanism was also studied by time-resolved measurements. According to the τ/τ_0 plots shown in Figure 4A, the lifetime of PA-2PhAn remains relatively stable with the exposure time in the NB vapor, which proves that it is a static quenching. The significant difference between τ/τ_0 and quenching efficiency is due to the formation of a non-fluorescent electron-transfer complex. The SAMs will be refreshed easily because of the low stability of the complex and weak bonding between the NAC and SAM surfaces.

Reversibility of the Quenching Process. Fluorescence intensities of the AIEE SAM sensor were recorded during the eight continuous tests. As shown in Figure S6, the quenching loss caused by tests excited at 263 nm is less than 10%, which proves the robustness of the SAM sensors. The reversibility of the SAM to NACs was conducted with pure NB. Emission spectra were recorded before and after exposure to a saturated NB vapor at room temperature for 5 min. Then, the films were refreshed by immersing them in ethanol for 5 min and the emission spectra were recorded again after their blow-drying. The reversibility was checked by repeating the processes several times. As shown in Figure 4B, the response of the Ph-2PhAn SAMs to the NB vapor had merely about 10% loss and tended to be stable after three cycles. It promotes the SAM to be a robust sensor in wearable applications.

Sensitivity of the SAM Sensors. As a living sensing layer, the SAMs have a very small thickness, and the device response is relatively high in low concentrations and fast in speed in comparison with that of the bulk materials. Fluorescence quenching tests of the silicon wafer device were conducted by immersing in a complete stable vapor of 50 μL of NAC solution of different concentrations in methanol for 10 s. As shown in Figure 4C, we found that the SAM was very sensitive in such a short time and the detection sensitivity followed the order trinitrotoluene (TNT) > dinitrotoluene (DNB) > NB at most concentrations. If the detection is considered to be effective when the fluorescence quenching efficiency with an exposure time of 10 s is higher than the upper limit of ethanol for 1 min (14.8%, Figure 4D), the detection limits of TNT, DNB, and NB are calculated according to eqs S2 and S3 as ~ 1.4 , ~ 8.4 , and ~ 249.5 ppm, respectively, enabling rapid detection of the NAC solution vapor. As the number of electron-withdrawing nitro groups increases, the electron-withdrawing capabilities of NB, DNB, and TNT increase sequentially. Therefore, the NACs with more nitro groups can form more stable complexes with PA-2PhAn in less time, and the difference will eventually be reflected in the fluorescence

quenching sensitivity. However, the SAM sensor should have a much lower detection limit with a pure NAC vapor that is commercially unavailable. The vapor of methanol liquefies immediately onto the SAM surface and takes the NAC molecules away again out of the apparatus, which undermines the sensitivity.

Selectivity of the SAM Sensors. The SAMs have good selectivity. Compared with that of the common chemical reagents, such as methanol, tetrahydrofuran, toluene, chlorobenzene, acetone, 1,2-dichloroethane, *n*-hexane, and formic acid, the fluorescence quenching efficiency of NB was found to be as high as 80% with an exposure time of 1 min in their saturated vapor. It shows selectivity in comparison with other chemical reagents mentioned above in Figure 4D.

CONCLUSIONS

To summarize, we present a novel self-assembled molecule PA-2PhAn, wherein 9,10-diphenyl anthracene is an AIEE fluorophore and phosphoric acid is used as an anchor group, linked to the fluorophore via an alkyl chain. A compact and dense SAM was formed by immersing the substrate with a HfO₂ layer into a solution of PA-2PhAn, and a NAC gas sensor was fabricated with the obtained SAMs based on fluorescence quenching. It was found that SAM exhibited high sensitivity to NACs at low solution concentrations, especially for TNT and DNT. Further examination showed that the responses of the SAMs to NACs were reversible, and their sensing performances were more efficient compared with those of the common interferents. The sensitivity, reversibility, and selectivity may qualify PA-2PhAn as promising NAC fluorescent sensor materials. Moreover, SAM molecules can be deposited on the surface of a flexible substrate to enable the fabrication of flexible NAC sensors. These devices offer opportunities for the preparation of flexible sensors and the development of wearable devices.

ASSOCIATED CONTENT

Supporting Information

The Supporting Information is available free of charge at <https://pubs.acs.org/doi/10.1021/acs.langmuir.9b03742>.

Molecular synthesis; X-ray photoelectron spectroscopy; X-ray reflectivity; contact angle; UV-vis absorption; fluorescence quenching and measurements; operation process for the quenching mechanism, reversibility, sensitivity, and selectivity in Figure 4; calculation of the detection limit; details of device fabrication and characterization (PDF)

AUTHOR INFORMATION

Corresponding Authors

Xuefeng Guo – Beijing National Laboratory for Molecular Sciences, State Key Laboratory for Structural Chemistry of Unstable and Stable Species, College of Chemistry and Molecular Engineering and Department of Materials Science and Engineering, College of Engineering, Peking University, Beijing 100871, P. R. China; orcid.org/0000-0001-5723-8528; Email: guoxf@pku.edu.cn

Hailing Tu – GRIMAT Engineering Institute Co., Ltd, Beijing 101407, P. R. China; State Key Laboratory of Advanced Materials for Smart Sensing, General Research Institute for Nonferrous Metals, Beijing 100088, P. R. China; Email: tuhl@grinn.com

Authors

Mingliang Li – GRIMAT Engineering Institute Co., Ltd, Beijing 101407, P. R. China; State Key Laboratory of Advanced Materials for Smart Sensing, General Research Institute for Nonferrous Metals, Beijing 100088, P. R. China; orcid.org/0000-0002-6181-5954

Hongliang Chen – Department of Chemistry, Northwestern University, Evanston, Illinois 60208, United States

Shuo Li – GRIMAT Engineering Institute Co., Ltd, Beijing 101407, P. R. China; State Key Laboratory of Advanced Materials for Smart Sensing, General Research Institute for Nonferrous Metals, Beijing 100088, P. R. China

Guozhi Wang – GRIMAT Engineering Institute Co., Ltd, Beijing 101407, P. R. China; State Key Laboratory of Advanced Materials for Smart Sensing, General Research Institute for Nonferrous Metals, Beijing 100088, P. R. China

Feng Wei – GRIMAT Engineering Institute Co., Ltd, Beijing 101407, P. R. China; State Key Laboratory of Advanced Materials for Smart Sensing, General Research Institute for Nonferrous Metals, Beijing 100088, P. R. China

Complete contact information is available at: <https://pubs.acs.org/10.1021/acs.langmuir.9b03742>

Author Contributions

[#]M.L. and H.C. contributed equally to this work. X.G. and M.L. conceived and designed the experiments. M.L. and H.C. performed material synthesis, device fabrication, and most of the device characterizations. S.L. and G.W. performed the XRR measurements. M.L., H.C., S.L., G.W., F.W., and X.G. analyzed the data and wrote the paper. All of the authors discussed the results and commented on the manuscript. All authors have given approval to the final version of the manuscript.

Funding

Financial support from the GRINM Youth Foundation, National Key R&D Program of China (2017YFA0204901), the National Natural Science Foundation of China (grants 21727806 and 21933001), the Natural Science Foundation of Beijing (Z181100004418003), the DFG Research Unit FOR 1979, the Tencent Foundation through the Xplorer Prize, and the Cluster of Excellence RESOLV (EXC-2033, Project number 390677874) is gratefully acknowledged. Thanks are due to Mr. Mingxing Chen for his help in fluorescence tests and discussions.

Notes

The authors declare no competing financial interest.

ABBREVIATIONS

AIEE, aggregation-induced emission enhancement; SAM, self-assembled monolayer; NACs, nitroaromatic compounds; HPLC, high-performance liquid chromatography; MS, mass spectrometry; ACQ, aggregation-caused quenching; XPS, X-ray photoelectron spectroscopy; XRR, X-ray reflectivity; AFM, atomic force microscopy; NB, nitrobenzene; TNT, trinitrotoluene; DNB, dinitrotoluene

REFERENCES

- (1) Giannoukos, S.; Brkic, B.; Taylor, S.; Marshall, A.; Verbeck, G. F. Chemical Sniffing Instrumentation for Security Applications. *Chem. Rev.* **2016**, *116*, 8146.
- (2) Sun, X. C.; Wang, Y.; Lei, Y. Fluorescence based explosive detection: from mechanisms to sensory materials. *Chem. Soc. Rev.* **2015**, *44*, 8019.

- (3) Kumar, V.; Maiti, B.; Chini, M. K.; De, P.; Satapathi, S. Multimodal Fluorescent Polymer Sensor for Highly Sensitive Detection of Nitroaromatics. *Sci. Rep.* **2019**, *9*, No. 7269.
- (4) Chhatwal, M.; Mittal, R.; Gupta, R. D.; Awasthi, S. K. Sensing Ensembles for Nitroaromatics. *J. Mater. Chem. C* **2018**, *6*, 12142.
- (5) Koudehi, M. F.; Pourmortazavi, S. M. Polyvinyl Alcohol/Polypyrrole/Molecularly Imprinted Polymer Nanocomposite as Highly Selective Chemiresistor Sensor for 2,4-DNT Vapor Recognition. *Electroanalysis* **2018**, *30*, 2302.
- (6) McQuade, D. T.; Pullen, A. E.; Swager, T. M. Conjugated polymer-based chemical sensors. *Chem. Rev.* **2000**, *100*, 2537.
- (7) Kim, Y.; Whitten, J. E.; Swager, T. M. High ionization potential conjugated polymers. *J. Am. Chem. Soc.* **2005**, *127*, 12122.
- (8) Zhou, Q.; Swager, T. M. Method for enhancing the sensitivity of fluorescent chemosensors: energy migration in conjugated polymers. *J. Am. Chem. Soc.* **1995**, *117*, 7017.
- (9) Yang, J.-S.; Swager, T. M. Porous Shape Persistent Fluorescent Polymer Films: An Approach to TNT Sensory Materials. *J. Am. Chem. Soc.* **1998**, *120*, 5321.
- (10) Zhang, S.; Lü, F.; Gao, L.; Ding, L.; Fang, Y. Fluorescent Sensors for Nitroaromatic Compounds Based on Monolayer Assembly of Polycyclic Aromatics. *Langmuir* **2007**, *23*, 1584.
- (11) He, G.; Zhang, G.; Lü, F.; Fang, Y. Fluorescent Film Sensor for Vapor-Phase Nitroaromatic Explosives via Monolayer Assembly of Oligo(diphenylsilane) on Glass Plate Surfaces. *Chem. Mater.* **2009**, *21*, 1494.
- (12) Ma, X. F.; Sun, R.; Cheng, J. H.; Liu, J. Y.; Gou, F.; Xiang, H. F.; Zhou, X. G. Fluorescence Aggregation-Caused Quenching versus Aggregation-Induced Emission: A Visual Teaching Technology for Undergraduate Chemistry Students. *J. Chem. Edu.* **2016**, *93*, 345.
- (13) Yamaguchi, M.; Ito, S.; Hirose, A.; Tanaka, K.; Chujo, Y. Control of aggregation-induced emission versus fluorescence aggregation-caused quenching by bond existence at a single site in boron pyridinoiminate complexes. *Mater. Chem. Front.* **2017**, *1*, 1573.
- (14) Forster, T.; Kasper, K. Ein Konzentrationsumschlag Der Fluoreszenz Des Pyrens. *Zeitschrift Fur Elektrochemie* **1955**, *59*, 976.
- (15) Mei, J.; Leung, N. L. C.; Kwok, R. T. K.; Lam, J. W. Y.; Tang, B. Z. Aggregation-Induced Emission: Together We Shine, United We Soar! *Chem. Rev.* **2015**, *115*, 11718.
- (16) Zeng, Q.; Li, Z.; Dong, Y. Q.; Di, C. A.; Qin, A. J.; Hong, Y. N.; Ji, L.; Zhu, Z. C.; Jim, K. W.; Yu, G.; Li, Q. Q.; Li, Z. G.; Liu, Y. Q.; Qin, J. G.; Tang, B. Z. Fluorescence enhancements of benzene-cored luminophors by restricted intramolecular rotations: AIE and AIEE effects. *Chem. Commun.* **2007**, 70.
- (17) Hu, R.; Leung, N. L. C.; Tang, B. Z. AIE macromolecules: syntheses, structures and functionalities. *Chem. Soc. Rev.* **2014**, *43*, 4494.
- (18) Chen, H.; Guo, X. Unique Role of Self-Assembled Monolayers in Carbon Nanomaterial-Based Field-Effect Transistors. *Small* **2013**, *9*, 1144.
- (19) Li, Q.; Yang, Z.; Ren, Z.; Yan, S. Polysiloxane-Modified Tetraphenylethene: Synthesis, AIE Properties, and Sensor for Detecting Explosives. *Macromol. Rapid Commun.* **2016**, *37*, 1772.
- (20) Chen, H.; Dong, S.; Bai, M.; Cheng, N.; Wang, H.; Li, M.; Du, H.; Hu, S.; Yang, Y.; Yang, T.; Zhang, F.; Gu, L.; Meng, S.; Hou, S.; Guo, X. Solution-Processable, Low-Voltage, and High-Performance Monolayer Field-Effect Transistors with Aqueous Stability and High Sensitivity. *Adv. Mater.* **2015**, *27*, 2113.
- (21) Smits, E. C. P.; Mathijssen, S. G. J.; van Hal, P. A.; Setayesh, S.; Geuns, T. C. T.; Mutsaers, K. A. H. A.; Cantatore, E.; Wondergem, H. J.; Werzer, O.; Resel, R.; Kemerink, M.; Kirchmeyer, S.; Muzafarov, A. M.; Ponomarenko, S. A.; de Boer, B.; Blom, P. W. M.; de Leeuw, D. M. Bottom-up organic integrated circuits. *Nature* **2008**, *455*, 956.
- (22) Schmaltz, T.; Amin, A. Y.; Khassanov, A.; Meyer-Friedrichsen, T.; Steinrück, H.-G.; Magerl, A.; Segura, J. J.; Voitkovsky, K.; Stellacci, F.; Halik, M. Low-Voltage Self-Assembled Monolayer Field-Effect Transistors on Flexible Substrates. *Adv. Mater.* **2013**, *25*, 4511.
- (23) Khassanov, A.; Steinrück, H.-G.; Schmaltz, T.; Magerl, A.; Halik, M. Structural Investigations of Self-Assembled Monolayers for Organic Electronics: Results from X-ray Reflectivity. *Acc. Chem. Res.* **2015**, *48*, 1901.
- (24) Zhang, B.; Kong, T.; Xu, W.; Su, R.; Gao, Y.; Cheng, G. Surface Functionalization of Zinc Oxide by Carboxyalkylphosphonic Acid Self-Assembled Monolayers. *Langmuir* **2010**, *26*, 4514.
- (25) Nandi, A.; Manna, B.; Ghosh, R. Interplay of exciton–excimer dynamics in 9,10-diphenylanthracene nanoaggregates and thin films revealed by time-resolved spectroscopic studies. *Phys. Chem. Chem. Phys.* **2019**, *21*, 11193.
- (26) Lakowicz, J. R. *Principles of Fluorescence Spectroscopy*, 2nd ed.; Kluwer Academic/Plenum: New York, 1999.